Available online at www.sciencedirect.com

ScienceDirect

IFAC Papers Online CONFERENCE PAPER ARCHIVE

IFAC PapersOnLine 55-6 (2022) 575–582

Fault quantifcation and mitigation method for energy management in microgrids using MPC reconfiguration.

J. J. Marquez * **A. Zafra-Cabeza** * **C. Bordons** *

* *Department of System Engineering and Automatic Control. Universidad de Sevilla. Escuela Superior de Ingeniería. Camino de los Descubrimientos, s/n 41092 Seville (SPAIN).(e-mail: jmarquez20@us.es; asunzafra@us.es; bordons@us.es*

Abstract: The current energy situation and the possibility of exhausting fossil fuels in a relatively near period, have led to investing efforts in the development of techniques that use renewable energy sources for power generation. A configuration that allows renewable energy sources to be integrated into the overall power system, advocates dividing the grid into distributed systems incorporating small-scale generation and storage. Microgrids are a well-known type of these systems. Control systems help maintain the reliability of the energy supply while minimizing costs. In addition, it must be taken into account that faults can occur in the processes that make up the microgrid. In some cases, the control system can mask these faults, even allowing the fault to reach an irreparable level. In this context, fault-tolerant control is a tool that enables control objectives to be maintained even in the presence of faults. If necessary, the control objectives are adapted to the fault. Furthermore, the fault tolerant control system needs to be able to detect faults, quantify their intensity and act accordingly. In this way it is avoided that small faults, that in other circumstances would remain hidden by the control loop, cause faults of a greater magnitude. This article proposes a fault quantification method based on parity equations and structured residuals that, together with a fault accommodation tolerance mechanism, mitigates the consequences of possible faults in this type of system.

Keywords: Microgrids, Model Predictive Control, Fault tolerant control, Fault quantification, Accommodation

1. INTRODUCTION

Alternatives to the current energy model are currently being sought in order to avoid climate change. A more environmentally friendly energy model must have renewable energy sources as the main energy resource. However, the generally fluctuating and intermittent nature of these types of power sources is holding back their integration. In this sense, the current research lines on microgrids, are focused on both generation, storage and consumption..

The term microgrid has been defined by different authors (Eto et al. (2018); Olivares et al. (2014); Hamdi et al. (2017)). In this paper, the following definition of microgrid has been adopted considering previous authors : a microgrid is a set of Distributed Energy Sources (DER), Energy Storage Systems (ESS) and electrical loads that operate together with management, control and protection systems to maintain supply quality and reliability while optimizing energy dispatch. Being able to work in isolation or connected to an external electrical grid through the Common Coupling Point (PCC).

Control systems are an essential part of the path that has been set for the integration of Renewable Energy Sources (RES) in the energy model. A review of the control strategies applied to microgrids can be seen in Olivares et al. (2014); Minchala-Avila et al. (2015). Where Model-based Predictive Control (MPC) is considered as a strategy widely used for microgrid control (Garcia-Torres et al. (2016, 2020); Bruni et al. (2015); Parisio et al. (2014); Pereira et al. (2015); Yan et al. (2019)). The Model-based Predictive Control (MPC) stands out for the relevant characteristics it presents compared to other control policies, such as the use of a model to predict the output, easy handling of constraints, weighting factors for the error and control effort and the incorporation of delays F. Camacho and Bordons (2007).

However, sometimes the control loop can hide low-level faults in the system, allowing that the fault can reach an unacceptable level before being detected. Fault Tolerant Control (FTC) allows diagnosing and mitigating the faults that have occurred and stopping the operation of the system if necessary. According to Escobet et al. (2019), FTC provides tools to maintain control objectives even in the presence of faults, admitting a certain degradation of their performance. In this paper, the FTC is studied from the point of view of the Energy Management System (EMS). M. Morato et al. (2020) present a fault tolerant

⋆ Ministerio de Ciencia e Innovación, Agencia Estatal de Investigación MCIN/AEI/ 10.13039/501100011033 under grant PID2019-104149RB-I00 (project SAFEMPC)

10.1016/j.ifacol.2022.07.190

power management that uses linear observers with varying parameters to carry out fault estimation. From the EMS point of view, in Marquez et al. (2020) an MPC is developed that mitigates the effects of previously diagnosed faults in a microgrid. Other more recent work for the FTC of an EMS is presented in Morato et al. (2021).

Within fault diagnosis, a well-known methodology is based on analytical redundancy with parity equations and structured residuals (Blanke et al. (2000); Isermann (2006)). A model-based approach is used in this work. Using an analytical redundancy relationship, the model and the process are compared at each sampling period; when inconsistencies between both signals are detected, the residuals take a non-zero value (Chow and Willsky (1984)). Note that sometimes the residual can be non-zero due to modeling uncertainties or errors, resulting in a false alarm fault. For this reason, it is necessary to establish thresholds that determine the occurrence of a fault. In a previous work by the authors, a novel design of the thresholds to reject false alarm faults was presented using random restrictions and historical residual signals with measurement and modeling errors characterized in a probabilistic way (Marquez et al. (2020)).

The combination of FTC strategies together with MPC approaches applied to microgrid energy management systems can be an interesting field to explore. However, this combination has not yet been widely studied. This work presents a stochastic fault diagnosis and isolation method based on parity equations to be integrated in the control loop, where a MPC is used to drive the microgrid to correct values. The stochastic property is given by probabilistic thresholds that are calculated in each time to decide if the values of outputs are in acceptable bounds or not.

In addition, a procedure to quantify the detected fault is incorporated to carry out the mitigation of the faults with more accuracy. The fault mitigation is undertaken considering the previous information and some matrices describing the reconfiguration actions to do.

The scope of this work encompasses the development of a MPC-based partial fault mitigation (FM) scheme that includes FDI and reconfiguration activities. The tests were carried out in MATLAB/Simulink Simugrid library (software companion of Bordons et al. (2020)). Therefore, the main contributions of this work are:

(a) The development of a method that quantifies the fault.
(b) The design of the formulation necessary to generate the mitigation actions that will be executed by the MPC.

The document has been organized as follows: Section 2 describes the real DC microgrid used as a case study, its components and the approximated linear model used for controller design. Section 3 describes the proposed Fault Tolerant Control strategy and how it is integrated together with the MPC in the control scheme. Section 4 shows the results of the simulations. Finally, Section 5 presents a discussion on the results obtained and future perspectives.

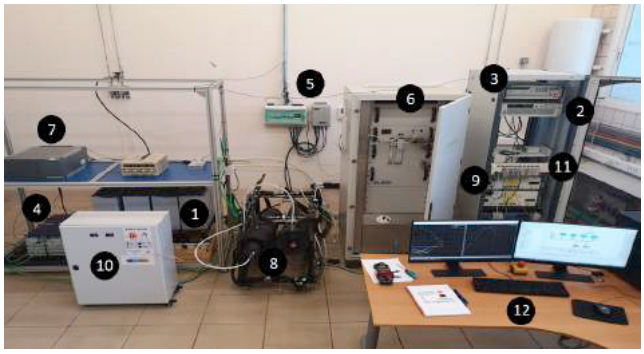

Fig. 1. Microgrid used as study case

2. DESCRIPTION OF THE REAL MICROGRID USED AS CASE STUDY

The simulations carried out in this work have been defined from a real DC microgrid located at the University of Seville. The microgrid is made up of a lead-acid battery bank, a lithium-ion battery bank, an electrolyzer, a metal hydride tank, a Proton Exchange Membrane Fuel Cells (PEMFC), a photovoltaic field, a programmable power source, an electronic load and several DC/DC converters. Table 1 shows devices specifications.

Table 1. Components of the microgrid.

Device	Nominal value
Programmable power supply	6kW
Photovoltaic field	4kW
Electronic load	1kW
Electrolyzer	$0.23Nm^3/h$ at 3kW
Metal hydride tank	$7Nm^3$ at 5bar
PEMFC	1.5kW at 20N
Lead-acid battery bank capacity	C_{120}=370Ah
Lithium battery bank capacity	400Ah

Fig. 1 shows of the microgrid sheme used. Being:

(1) Lead acid battery bank.
(2) Programmable power supply.
(3) Lithium-ion battery bank.
(4) Photovoltaic field.
(5) Electrolyzer.
(6) PEMFC.
(7) Metal hydrides tank.
(8) PEMFC DC/DC.
(9) Lithium-ion battery DC/DC.
(10) PLC.
(11) Workstation.

The lead battery is used to regulate the voltage of the power bus. This bus is rated at 48 volts. Lithium batteries are usually the most affected by operations carried out in the microgrid. The generation and demand profiles used to carry out the simulation have been obtained from the page of Red Electrica de España (https://demanda.ree.es/movil/peninsula).

2.1 Model of the microgrid

Since the energy management strategy used is based on MPC, a model is developed in state space. At this level of control, only the dynamics of the Energy Storage Systems

is taken into account. The discrete equations of the control-oriented model are obtained from:

$$SOC_{le}(t+1) = SOC_{le}(t) - \frac{\eta_{le} T_s}{C_{le}^{max}} P_{le}(t) \quad (1)$$

$$SOC_{li}(t+1) = SOC_{li}(t) - \frac{\eta_{li} T_s}{C_{li}^{max}} P_{li}(t) \quad (2)$$

$$LOH(t+1) = LOH(t) - \eta_{H_2} T_s P_{H_2}(t) \quad (3)$$

and from the balance equation:

$$P_{dem}(t) = P_{le}(t) + P_{li}(t) + P_{H2}(t) + P_{grid}(t) + P_{res}(t) \quad (4)$$

where SOC_{le} and SOC_{li} are the charge levels of the batteries and LOH is the Level of Hydrogen. T_s indicates the sampling time, η (considered as an average efficiency between loading and unloading) represents the efficiency parameter that depends on the operating point and C^{max} represents the capacity of the ESSs in units of energy. P_{le}, P_{li}, P_{H2} and P_{grid} are the energy provided/absorbed by the lead-acid battery, the lithium-ion battery, the metal hydrides and the distribution grid respectively. P_{dem} is the power of demand and P_{res} the power generated by renewable sources.

The difference between the generated power and the demanded power is considered a disturbance called P_{net} ($P_{net} = v$), it is expressed as:

$$P_{net}(t) = P_{res}(t) - P_{dem}(t) \quad (5)$$

From the above, the control-oriented model is defined as:

$$SOC_{le}(t+1) = SOC_{le}(t) - K_{le} T_s (-P_{li}(t) - P_{H2}(t) - P_{grid}(t) - P_{net}(t)) \quad (6)$$

$$SOC_{li}(t+1) = SOC_{li}(t) - K_{li} T_s P_{li}(t) \quad (7)$$

$$LOH(t+1) = LOH(t) - K_{H2} T_s P_{H_2}(t) \quad (8)$$

and the model in state variables:

$$x(t+1) = Ax(t) + Bu(t) + Ev(t) \quad (9)$$

$$y(t) = Cx(t) \quad (10)$$

where $x = [SOC_{le}\ LOH\ SOC_{li}]^T$ is the vector of states and represents the energy stored in the different Energy Storage Systems, $u = [P_{H2}\ P_{grid}\ P_{li}]^T$ is the vector of manipulated variables. Sign criterion has been chosen in which the energy contribution to power bus has positive sign, otherwise negative value.

2.2 Constraints

The operating constraints that guarantee the safe operation of the plant must be taken into account. There are physical thresholds that cannot be crossed in any case, the constraints prevent these thresholds from being crossed.

The hard constraints of the control variables are:

$$\begin{array}{rcl} -2.9\,kW \leq & P_{H2}(t) & \leq 1.2\,kW \\ -2.5\,kW \leq & P_{grid}(t) & \leq 6\,kW \\ -3\,kW \leq & P_{li}(t) & \leq 3\,kW \\ -1.0\,kW \leq & \triangle P_{H2}(t) & \leq 1.0\,kW \\ -1.0\,kW \leq & \triangle P_{grid}(t) & \leq 1.0\,kW \\ -1.0\,kW \leq & \triangle P_{li}(t) & \leq 1.0\,kW \end{array} \quad (11)$$

The constraints regarding the level of charge are shown below:

$$\begin{array}{l} 40\,\% \leq SOC_{le}(t) \leq 75\,\%, \\ 10\,\% \leq LOH(t) \leq 95\,\%, \\ 30\,\% \leq SOC_{li}(t) \leq 80\,\% \end{array} \quad (12)$$

3. FAULT TOLERANT ENERGY MANAGEMENT SYSTEM

The energy management system has been carried out by means of a model-based predictive control. The MPC must allow the necessary control signals to be calculated at each sampling time to achieve optimal use of the microgrid resources taking into account the operating constraints.

The general control objectives are summarized below:

(a) Facilitate the application of constraints
(b) Optimize resources by minimizing the exchange of energy between equipment
(c) Minimize variations in bus voltage
(d) Allow operational flexibility of lithium batteries and minimize the use of the distribution grid.

Also, from the point of view of the FTC, the optimization should be taken into account even if changes have appeared in the plant as a result of faults.

The Pareto optimum of this multiobjective problem is solved by satisfying the standard objective function J:

$$J(x(t), u(t)) = (x(t) - x_{ref}(t))^T \delta (x(t) - x_{ref}(t)) + \\ + \Delta u^T(t) \lambda \Delta u(t) + u^T(t) \alpha u(t) \quad (13)$$

which is solved for each instant of time by:

$$\min_{\{u(t),\ldots,u(t+N-1)\}} \sum_{i=0}^{N-1} J(x(t+i), u(t+i)), \quad (14)$$

subject to

$x(t+1)=Ax(t)+Bu(t)+Ev(t), \quad \forall t \in Z_0^{N-1}$,
$x(0) = x(t)$,
$x(t+1) \in \mathcal{X}, \quad \forall t \in Z_0^{N-1}$,
$u(t) \in \mathcal{U}, \quad \forall t \in Z_0^{N-1}$,
$v(t) \in \mathcal{V}, \quad \forall t \in Z_0^{N-1}$

Initially, a setpoint (reference charging level) is established for each energy storage system. The first term in (13) sets the flexibility of each team with respect to the initial set point.

3.1 Fault Mitigation Module (FMM)

This module is responsible for the fault diagnosis, isolation and mitigation. The FMM receives as inputs the plant outputs (y), the controller outputs (u), the historical values of the system variables (h_1), the disturbances and the noise signals (v) (see Fig. 2). Based on this information, the FMM module examines the occurrence of faults and, in the case of a fault, returns the mitigation actions (u^a) to be executed. In this work, mitigation actions are considered as adjustments on the parameters of the MPC.

The functionalities of the FMM are described below.

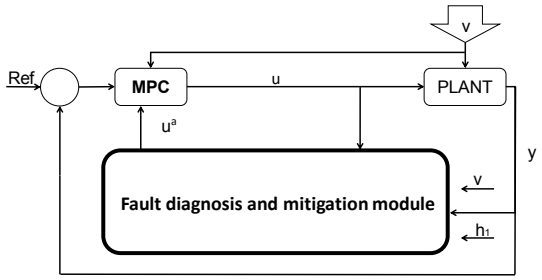

Fig. 2. General diagram of the FTC strategy developed

3.2 Approach for diagnosis and quatification of faults

To develop an effective FTC procedure, a detection algorithm has been designed together with a passive robustness method. For this, the uncertainty originated in the residual generation is assumed and the thresholds that must be exceeded are optimized to consider the existence of faults, using concepts of stochastic systems. In summary, to calculate the thresholds $[\gamma(t),\ \beta(t)]$, a set of historical experimental data in non-fault scenarios is used (see h_1 in fig. 2). These data are collected at the plant and used to obtain the probability density function. Time-varying stochastic thresholds are generated at each sampling time using probability constraints Kall and Wallace (1994). Mathematically, the problem can be stated as:

$$\begin{aligned} &max\ \gamma_i(t) \qquad\qquad s.t. \\ &P\{r_i^h(t) \geq \gamma_i(t)\} \geq 1-p,\ \forall i\ \forall t \end{aligned} \tag{15}$$

$$\begin{aligned} &min\ \beta_i(t) \qquad\qquad s.t. \\ &P\{r_i^h(t) \leq \beta_i(t)\} \leq p,\ \forall i\ \forall t \end{aligned} \tag{16}$$

where P is the probability distribution, r_i^h the historical values of the residual i, γ_i represents the upper threshold of the residual r_i, β_i the lower threshold and p represents the probability.

In a previous paper of the authors (Marquez et al. (2020)) of detection and isolation process of the fault is shown in an extensive way and with experimental results. This work is focused on the method used to quantify the detected fault.

Once the fault has been detected and isolated, it is necessary to quantify its size to provide more information about it, and act accordingly. In this study, three types of faults are distinguished based on their size:

(1) Total fault equal to 100%. It causes a total equipment or subsystem fault. Therefore, it is a critical fault. For example, the breakage of a conductor or fuse in the connection of the converter of the lithium ion batteries with the power bus causes that the batteries cannot be used.
(2) Fault less than 100% and greater than 40%. It is a severe partial fault of an equipment or subsystem. For example, partial fault of the inverter that connects the microgrid with the electrical distribution grid. (see Antunes et al. (2020)).
(3) Fault less than 40%. It is a moderate partial fault of an equipment or subsystem.

The method developed in this study to evaluate the size of the fault consists of calculating new residual signals, named virtual residuals r_i^a. These variables are calculated by obtaining the difference between (i) a virtual critical fault occurred and (ii) the real value of the residual at each sample time, so that:

$$r_i^a(t) = y_i^{100\%}(t) - \hat{y}(t) \tag{17}$$

where $r_i^a(t)$ is the virtual residual, $y_i^{100\%}$ is the value at this operation point of the output i when a critical fault was simulated and $\hat{y}$ is the estimated out value for that operating point. Note that residuals variables r_i are calculated by considering the real values of the outputs of the microgrid at time t, through:

$$r(t) = WY(t) - [WT_uU(t) + WT_vV_1(t) + WT_ff(t)] \tag{18}$$

where T_u, T_v and T_u are Toeplitz matrices, $Y(t)$ are the output of the process, $U(t)$ are the controlled input, $V(t)$ are the disturbances and $f(t)$ is the additive fault vector. Matrix W is used so that the residual does not depend on the state (see Marquez et al. (2018); Escobet et al. (2019); Marquez et al. (2020)).

This process is carried out for each sampling time. After that, the severity of the type is obtained through the variable T, according that:

$$\begin{aligned} &if\ 100\frac{r_i}{r_i^a} = 100 \qquad then\ T=1 \\ &if\ 40 <= 100\frac{r_i}{r_i^a} < 100 \ then\ T=2 \\ &if\ 100\frac{r_i}{r_i^a} < 40 \qquad then\ T=3 \end{aligned} \tag{19}$$

Therefore, if $T=1$, the fault is classified as critical, with $T=2$ is a severe fault and with $T=3$, the fault is considered as moderate.

Finally, the vector $f(t) \in [0,1]^{n_f}$ is generated, with n_f the number of faults. This vector informs about the detected faults at time t. Thus, if $f_i(t)=1$, the fault F_i has been detected and $f_i(t)=0$ otherwise.

The variable f is used for the mitigation, which is described in next section.

A simulation that implements this method is shown in section 4.

3.3 Approach for fault mitigation

This section develops an active mitigation strategy that make adjustments on the parameters of the MPC that drives the microgrid. To achieve the objectives it is necessary to use different tolerance mechanisms. The methods implemented here can be classified as:

(1) Accommodation to fault: it will be applied in the case of severe or moderate faults (T=2 and T=3, respectively).
(2) Reconfiguration against fault: it will be applied in the case of a critical fault (T=1).

Both accommodation and reconfiguration mechanisms are carried out by varying the constraints and weighting factors of the objective function considered as mitigation actions. These parameters are initially set after studying the effects of each fault.

To determine the actions to be taken for each fault, matrices $G \in \{0,1\}^{(n_f \times n_a)}$ and $H \in R^{(3n_f \times n_a)}$ are defined with n_f the number of total faults and n_a the total number of proposed mitigation actions. Matrix G represents the actions to be executed for each fault taking into account that if element $G_{ij} = 1$ then the fault F_i can be mitigated by the corresponding mitigation action A_j. On the other hand, matrix H states the magnitude of the mitigation actions. Therefore, the mitigation actions to do when fault F_i has been detected, are determined by:

$$u^a = G^i \otimes H^i \tag{20}$$

with G^i and H^i the vectors of the $i-th$ and $((i-1)*3+T_i)-th$ rows of matrices G and H, respectively. T_i is the severity of the fault and $\otimes$ the Schur product. The magnitude of the control actions defined in matrix H are established according to the vathe value of T_i and operational constraints. It is convenient to clarify that in case of multiple faults, only the mitigation actions linked to the fault with the highest priority will be carried out. Note that the number of rows in H is $3nf$ because the magnitud of the actions to apply depends on the severity of the fault.

Examples of these actions, matrices G and H will be shown in the next section.

4. RESULTS

This section shows the results obtained by applying the methods outlined above. First, the result obtained from applying the method developed to quantify the size of the fault without applying any tolerance mechanism is shown. After, results with mitigation are shown.

4.1 Results of the fault size quantification method

The generation and demand profiles given by Fig. 3 are considered. In this case, an artificially fault with a magnitude of 58% is considered.

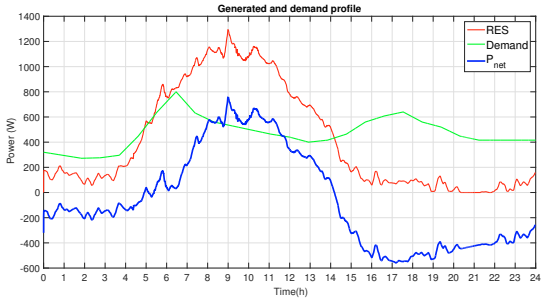

Fig. 3. Generation and demand profiles.

Until the moment of fault, the microgrid behaves correctly. The fault occurs at 10:00 am. Lithium batteries are expected to meet the demand required by the controller; however, the demand is not fully satisfied. The SOC_{le}

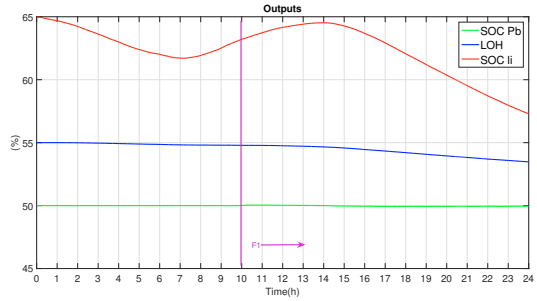

Fig. 4. ESSs load level in a fault scenario in P_{li} and without mitigation.

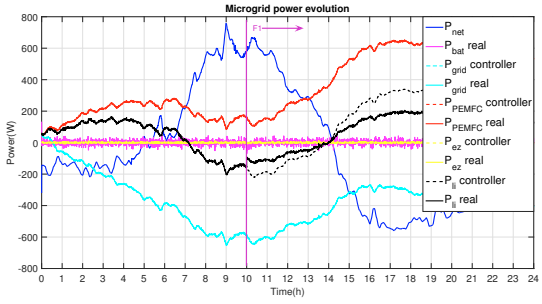

Fig. 5. Inputs in a fault scenario in P_{li} and without mitigation.

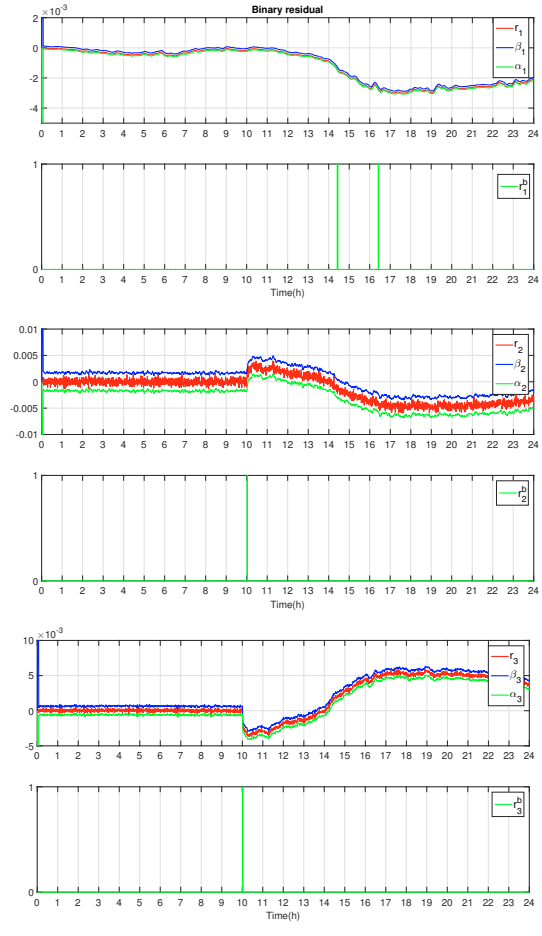

Fig. 6. Residual signals, thresholds and binary residuals in a P_{li} fault scenario and without mitigation.

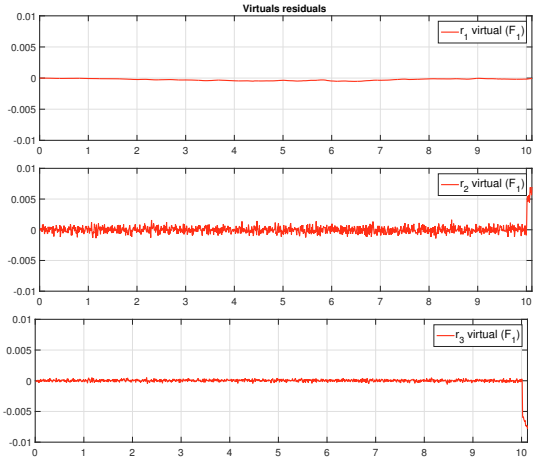

Fig. 7. Residual signals for a virtual 100% fault in P_{li}.

of the lead battery changes slightly after the fault (see Fig. 4). In this case the partial absence of P_{li} is satisfied by P_{H2} and P_{grid} (see Fig. 5). As can be observed, the input P_{li} (solid black line) does not follow the set point sent by the controller P_{li} *Controller* (black dotted line). Figure 6 shows the generated r_i residuals, the thresholds β_i, γ_i calculated using the passive robustness method and the binary residuals r_i^b (when r_i exceeds any threshold implies $r_i^b = 1$, see Fig. 6). The thresholds β_i and γ_i are calculated with a confidence interval of 95% (see Marquez et al. (2020). In this case, the residuals r_2 and r_3 go out of range when the fault occurs. Therefore, $r_1^b = 0$, $r_2^b = 1$ and $r_3^b = 1$ which means that the fault has occurred in the lithium batteries and therefore, $f_1 = 1$.

To provide information on the size of the fault, Fig 7 shows the virtual residuals calculated in open loop at the time of the actual fault (considered as 100% fault). It can be seen as the virtual residual $r_2^a \simeq 0.0065$ while the real residual $r_2 \simeq 0.0035$. With these values, the evaluation method determines a partial fault of approximately 54% (close to the 58% fault caused). On the other hand, through the remainder r_3 (virtual and real) a partial fault of 51% is determined. Therefore, it can be concluded that there is a partial fault of less than 100% and greater than 40%, therefore The fault F_1 is considered as severe and $T_1 = 2$.

4.2 Results of applying the fault accommodation mechanism

The mitigation actions considered for the accommodation case, as well as the G and H matrices for this case are defined below:

(1) a_1: changes the value of the upper limit of the SOC_{le}.
(2) a_2: changes the value of the lower limit of the SOC_{le}.
(3) a_3: changes the value of the upper limit of the LOH.
(4) a_4: changes the value of the lower limit of the LOH.
(5) a_5: changes the value of the upper limit of the SOC_{li}.
(6) a_6: changes the value of the lower limit of the SOC_{li}.
(7) a_7: change the value of the weighting factor δ for SOC_{le}.
(8) a_8: change the value of the weighting factor δ for SOC_{li}.
(9) a_9: change the value of the weighting factor δ for LOH.
(10) a_{10}: change the value of the weighting factor α for P_{le}.
(11) a_{11}: change the value of the weighting factor α for P_{H2}.
(12) a_{12}: change the value of the weighting factor α for P_{li}.

$$G = [\,0\;0\;0\;0\;0\;0\;1\;0\;0\;0\;0\;1\,] \tag{21}$$

$$H = \begin{bmatrix} 0 & 0 & 0 & 0 & 0 & 0 & 0 & 0 & 0 & 0 & 0 & 0 \\ 75 & 40 & 95 & 10 & 80 & 30 & 10^{-1} & 10^{-5} & 10^{-5} & 5\cdot10^{-5} & 10^{-3} & 5\cdot10^{-3} \\ 0 & 0 & 0 & 0 & 0 & 0 & 0 & 0 & 0 & 0 & 0 & 0 \end{bmatrix} \tag{22}$$

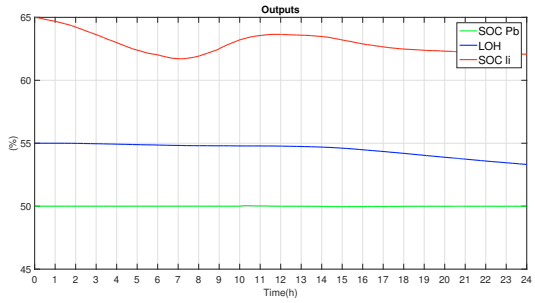

Fig. 8. Charge level of ESSs in a fault scenario in P_{li} with accommodation to fault.

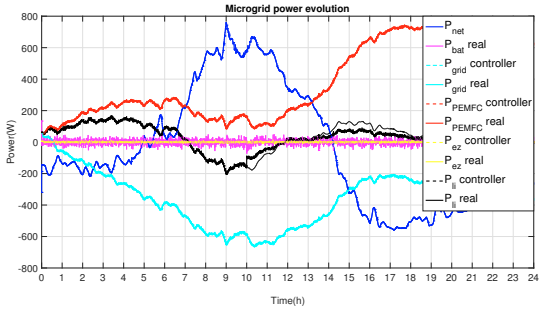

Fig. 9. Inputs of the control variables in a fault scenario in P_{li} with accommodation to fault.

The accommodation made in this case consists of increasing the weighting factor α corresponding to the lithium battery (a_7) to reduce its use. Due to the accommodation mechanism, the use of lithium batteries decreases (see Fig. 9).

When comparing P_{li} with P_{li} *Controller* in Fig. 9 it is observed that the fault still exists. However, the consumption of the distribution grid remains practically the same and the demand is satisfied.

Figure 10 shows the residuals r_i. The thresholds β_i and γ_i are calculated with a 95 % confidence interval using the hybrid method.

5. CONCLUSION

This work presents a novel MPC strategy to quantify and mitigate faults. The innovation consists of using virtual residual to quantify and mitigate fault through reconfiguration actions which are adjustments on the MPC. This document can be treated as an extension of a previous work Marquez et al. (2020). This framework makes possible to detect all faults (total or partial) if parameters of the stochastic algorithm are chosen appropriately.

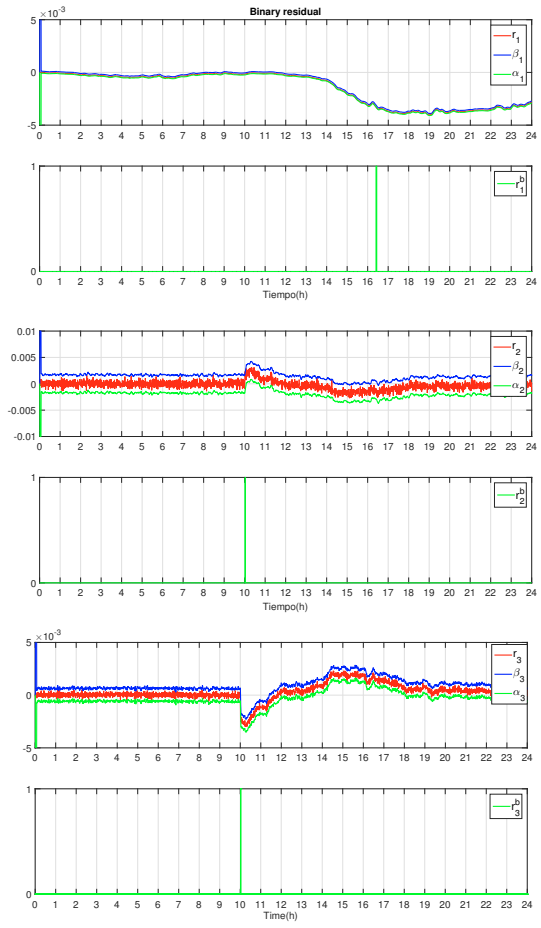

Fig. 10. Residual signals, thresholds and binary residuals in a fault scenario in P_{li} with accommodation to fault

The efficient isolation and quantification method of faults allows carry out the reconfiguration actions to drive the system to a safe state in a fault scenario.

To illustrate these results, a set of simulations has been implemented. The results obtained show the benefits of calculating the severity of faults and according that, determining the actions to mitigate it.

ACKNOWLEDGEMENTS

Grant PID2019-104149RB-I00 funded by MCIN/AEI/ 10.13039/501100011033.

REFERENCES

Antunes, H., Silva, S., Brandao, D., Machado, A., and Ferreira, V. (2020). A fault-tolerant grid-forming converter applied to ac microgrids. *International Journal of Electrical Power and Energy Systems*, 121.

Blanke, M., Frei, W., Patton, J., and Staroswiecki, M. (2000). What is fault-tolerant control? *IFAC Proceedings Volumes*, 33(11), 41–52.

Bordons, C., Garcia-Torres, F., and Ridao, M.A. (2020). *Model Predictive Control of Microgrids*. Springer.

Bruni, G., Cordiner, S., Mulone, V., Rocco, V., and Spagnolo, F. (2015). A study on the energy management in domestic micro-grids based on model predictive control strategies. *Energy Conversion and Management*, 102, 50–58.

Chow, E. and Willsky, A. (1984). Analytical redundancy and the design of robust failure detection systems. *IEEE Transactions on Automatic Control*, 7(29).

Escobet, T., Bregon, A., Pulido, B., and Puig, V. (2019). *Fault Diagnosis of Dynamic Systems, Quantitative and Qualitative Approaches*. Springer.

Eto, J., Lasseter, R., Klapp, D., Khalsa, A., Schenkman, B., Illindala, M., and Baktiono, S. (2018). The certs microgrid concept, as demonstrated at the certs/aep microgrid test bed.

F. Camacho, E. and Bordons, C. (2007). *Model Predictive Control. Second Edition*. Springer-Verlag, London, England.

Garcia-Torres, F., Vazquez, S., Bordons, C., Moreno-Garcia, I., Gil, A., and Roncero-Sanchez, P. (2020). Power quality management of interconnected microgrids using model predictive control. In *International Federation on Automatic Control World Congress 2020*.

Garcia-Torres, F., Valverde, L., and Bordons, C. (2016). Optimal load sharing of hydrogen-based microgrids with hybrid storage using model-predictive control. *IEEE Transactions on Industrial Electronics*, 63(8).

Hamdi, A., Beigvand, S., and La Scala, M. (2017). A review of optimal power flow studies applied to smart grids and microgrids. *Renewable and Sustainable Energy Reviews*, 71, 742–766.

Isermann, R. (2006). *Fault-Diagnosis Systems. An Introduction from Fault Detection to Fault Tolerance*. Springer.

Kall, P. and Wallace, S. (1994). *Stochastic Programming, First Edition*. Springer.

M. Morato, M., Mendes Paulo, R., Normey-Rico, J.E., and Bordons, C. (2020). Lpv-mpc fault-tolerant energy management strategy for renewable microgrids. *International Journal of Electrical Power and Energy Systems*, 117, 105644.

Marquez, J.J., Zafra-Cabeza, A., Bordons, C., and Ridao, M.A. (2020). A fault detection and reconfiguration approach using mpc for an experimental microgrid. *control engineering practice (CEP)*.

Marquez, J., Zafra-Cabeza, A., and Bordons, C. (2018). Diagnosis and fault mitigation in a microgrid using model predictive control. In *International Conference on Smart Energy Systems and Technologies (SEST)*. IEEE.

Minchala-Avila, L.I., Garza-Castanon, L.E., Vargas-Martinez, A., and Zhang, Y. (2015). Hybrid adaptive fault-tolerant control algorithms for voltage and frequency regulation of an islanded microgrid. *Procedia Computer Science*, 52, 827–844.

Morato, M.M., Vergara-Dietrich, J., Esparcia, E.A., Ocon, J.D., and Normey-Rico, J.E. (2021). Assessing demand compliance and reliability in the philippine off-grid islands with model predictive control microgrid coordination. *Renewable Energy*, 179(3).

Olivares, D.E., Mehrizi-Sani, A., Etemadi, A.H., Cañizares, C.A., Iravani, R., Kazerani, M., Hajimiragha, A.H., Gomis-Bellmunt, O., Saeedifard, M., Palma-Behnke, R., Jimenez-Estevez, G., and Hatziargyriou, N. (2014). Trends in microgrid control. *IEEE Transactions on Smart Grid*, 5(4), 1905–1919.

Parisio, A., Rikos, E., Tzamalis, G., and Glielmo, L. (2014). Use of model predictive control for experimental

microgrid optimization. *Applied Energy*, 115, 37–46.
Pereira, M., Limón, D., Muñoz de la Peña, D., Valverde, L., and Alamo, T. (2015). Periodic economic control of a nonisolated microgrid. *IEEE Transactions on Industrial Electronics*, 62(8), 5247–5255.
Yan, Z., Fanlin, M., Rui, W., Behzad, K., and Jianmai, S. (2019). Uncertainty-resistant stochastic mpc approach for optimal operation of chp microgrid. *Energy*, 179, 1265–1278.

Appendix A. A SUMMARY OF NOMENCLATURE

Table A.1. Table of symbols.

Acronyms	Description
DER	Distributed Energy Sources
ESS	Energy Storage Systems
PCC	Common Coupling Point
RES	Renewable Energy Systems
MPC	Model Predictive Control
FTC	Fault Tolerant Control
EMS	Energy Management System
FDB	Fault Diagnosis Block
FMB	Fault Mitigation Block
FMM	Fault Mitigation Module
Symbols	**Description**
SOC	State of Charge
LOH	Level of Hydrogen
le	Lead-acid battery.
li	Lithium-ion battery.
H_2	Hydrogen
η	simplified efficiency for the battery.
C	battery capacity in energy units.
T_s	sampling time.
K	conversion coefficient for the battery.
J	Objective function
x	State vector
u	Control (or input) vector
v	Disturbance vector
y	Output vector
A	State matrix
B	Input matrix
E	Disturbance matrix
C	Output matrix
δ	Weighting factor setpoint tracking.
λ	Weighting factor of efforts to increase control.
α	Weighting factor control effort.
r_i	Residual signal i.
r_i^h Historical residual	
r_i^a	Virtual residual signal i.
β	Upper stochastic threshold.
γ	Lower stochastic threshold.
u^a	Mitigation action.
H	Matrix indicating the magnitude of u^a.
G	Matrix that indicates the u^a to be executed.